Energy–Energy Correlator in the Regge Limit

Hongyi Ruan
Peking University

Work with Xiaoyuan Zhang, Hua Xing Zhu

SCET 2026 Workshop, KIAS

March 4, 2026

Energy Flow Operators and EEC

electron–positron colliders

[Basham, Brown, Ellis, Love, 1978]

introduced **energy–energy correlator**

$$\frac{d^2\Sigma}{d\Omega_a\, d\Omega_b} = \sum_{i,j} \int d\sigma\, \frac{E_i\, E_j}{Q^2}\, \delta^{(2)}(\Omega_a - \Omega_{p_i})\, \delta^{(2)}(\Omega_b - \Omega_{p_j})$$

as correlation of two energy detectors at spatial infinity (celestial sphere).

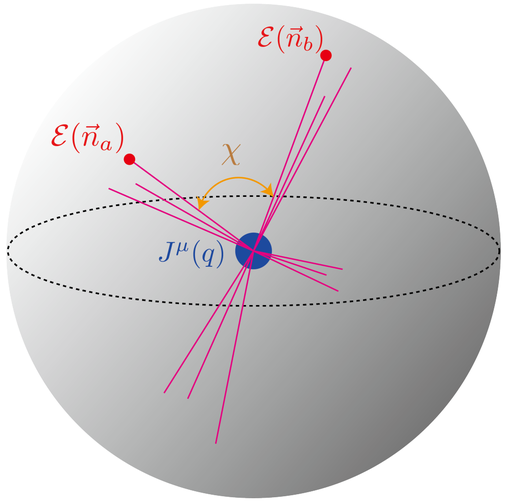

[Korchemsky, Sterman, 1999; Hofman, Maldacena, 2008; Bauer, Fleming Lee, Sterman, 2008; ...]

Also see Aditya Pathak's talk

$$\mathcal{E}(\vec{n}) = \lim_{r\to\infty} r^2 \int_0^\infty dt\; n^i\, T^{0i}(t, r\vec{n})$$

energy flow operator

in free theory

$$\mathcal{E}(\vec{n}) = \int \widetilde{d^3p}\, E_p\, a_p^\dagger a_p\, \delta^{(2)}\,(\vec{n} - \vec{n}_p)$$

Ensure soft and collinear safety!

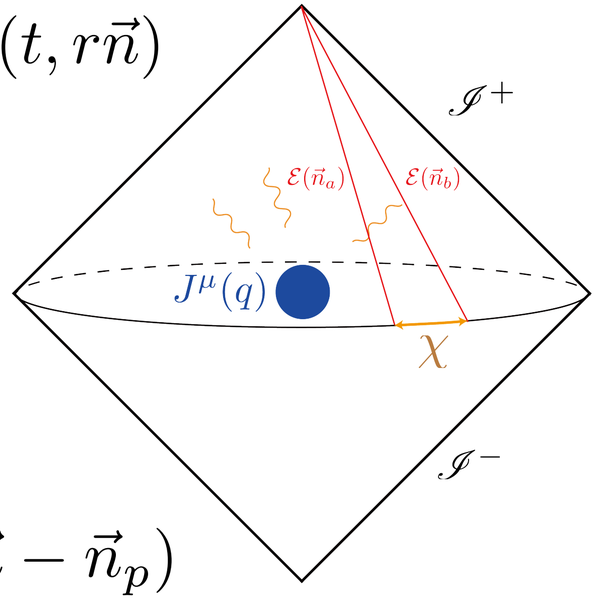

EEC at Hadron Colliders

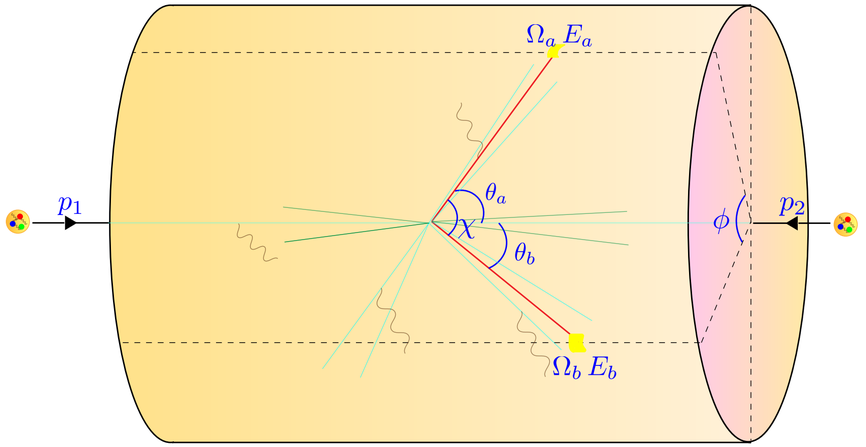

[Chen, HR, Zhu, 2025] generalize EEC to hadron collisions by considering hadronic initial states:

$$\frac{d^2\Sigma_H}{d\Omega_a\, d\Omega_b} = \frac{1}{2s_H} \frac{\langle P_1 P_2 \,|\mathcal{E}(n_a)\mathcal{E}(n_b)|\, P_1 P_2\rangle}{\langle P_1 P_2 | P_1 P_2\rangle}$$

In the hadron c.m. frame, the detector configuration is fully specified by $(Y, \Delta Y, \phi)$, with Y and ΔY the rapidity sum and separation of the two detectors,
and ϕ their azimuthal angel difference.

For later convenience: $\Delta_\eta = e^{\Delta Y}, \eta = e^{Y}$

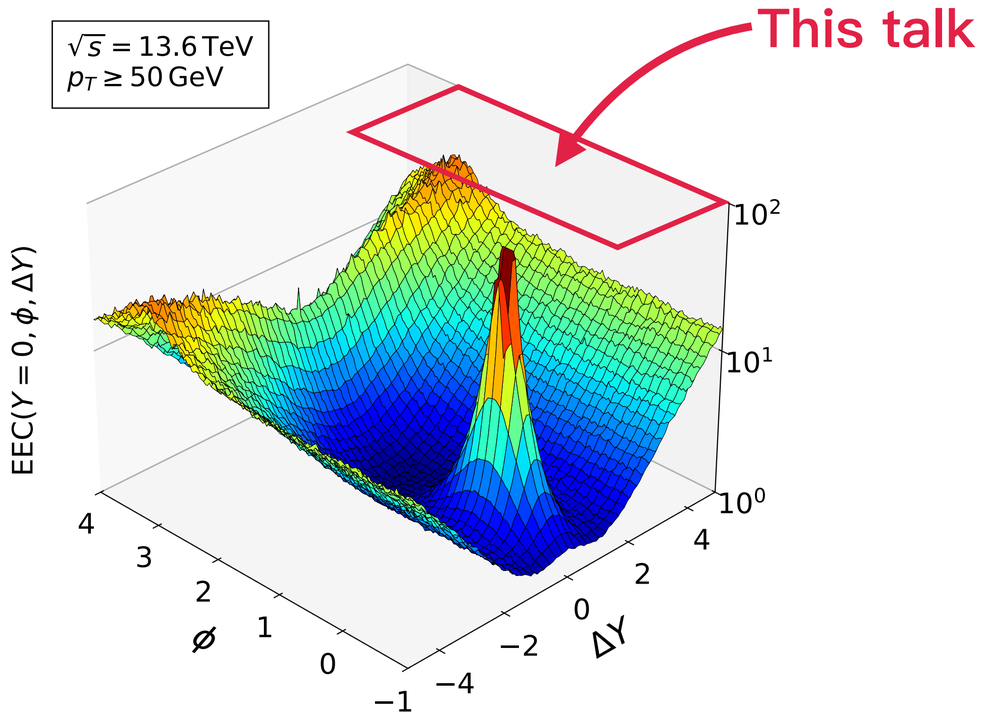

Pythia simulation of EEC for proton collisions

Aside: Related Work

- [Herrmann, Kologlu, Moult, 2412.05384] performed a similar perturbative quantum **gravity** calculation with two incoming scalars and highlighted several future directions.

Aside: Related Work

- [Herrmann, Kologlu, Moult, 2412.05384] performed a similar perturbative quantum **gravity** calculation with two incoming scalars and highlighted several future directions.
- [Chicherin, Korchemsky, Sokatchev, Zhiboedov, 2512.23791] extended the setup to **pure gravity and supergravity**, addressing contact terms and IR cancellations, derived an all–order expression in the back–to–back limit governed by universal soft–graviton dynamics, and introduced the ***beam-averaged EEC***.

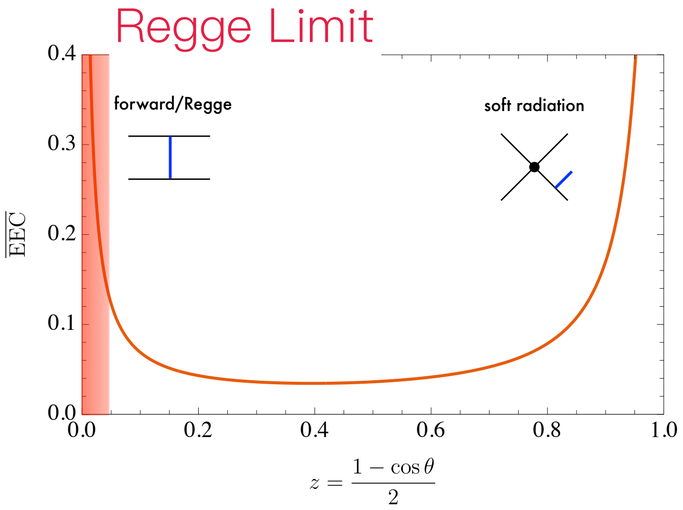

LO beam–averaged EEC of SUGRA

Aside: Related Work

- [Herrmann, Kologlu, Moult, 2412.05384] performed a similar perturbative quantum **gravity** calculation with two incoming scalars and highlighted several future directions.
- [Chicherin, Korchemsky, Sokatchev, Zhiboedov, 2512.23791] extended the setup to **pure gravity and supergravity**, addressing contact terms and IR cancellations, derived an all–order expression in the back–to–back limit governed by universal soft–graviton dynamics, and introduced the ***beam-averaged EEC***.
- [HR, Zheng, Zhu, 2601.21852] further generalized the construction by defining the ***celestial EEC*** with boost–eigenstate initial states, which takes the form of a 4pt function in a fictitious $2d$ CFT on the celestial sphere. We computed it in **(super) Yang–Mills and (super)gravity**, and showed that the $\mathcal{N}=8$ supergravity result can be **bootstrapped**.

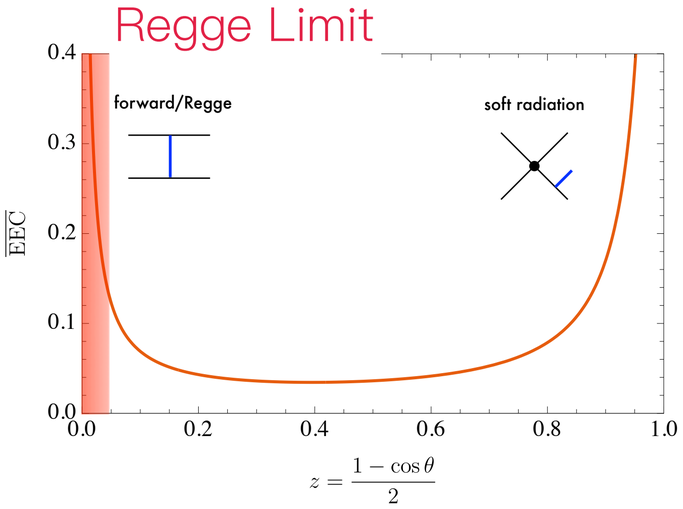

LO beam–averaged EEC of SUGRA

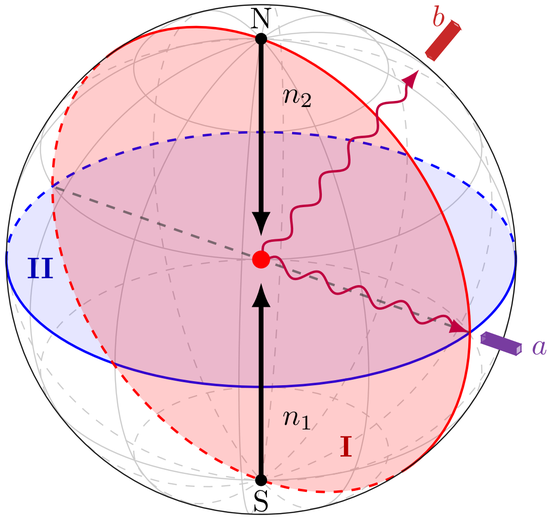

Lorentz symmetry helps fix three directions

Aside: Related Work

- [Herrmann, Kologlu, Moult, 2412.05384] performed a similar perturbative quantum **gravity** calculation with two incoming scalars and highlighted several future directions.
- [Chicherin, Korchemsky, Sokatchev, Zhiboedov, 2512.23791] extended the setup to **pure gravity and supergravity**, addressing contact terms and IR cancellations, derived an all–order expression in the back–to–back limit governed by universal soft–graviton dynamics, and introduced the ***beam-averaged EEC***.
- [HR, Zheng, Zhu, 2601.21852] further generalized the construction by defining the ***celestial EEC*** with boost–eigenstate initial states, which takes the form of a 4pt function in a fictitious $2d$ CFT on the celestial sphere. We computed it in **(super) Yang–Mills and (super)gravity**, and showed that the $\mathcal{N}=8$ supergravity result can be **bootstrapped**.

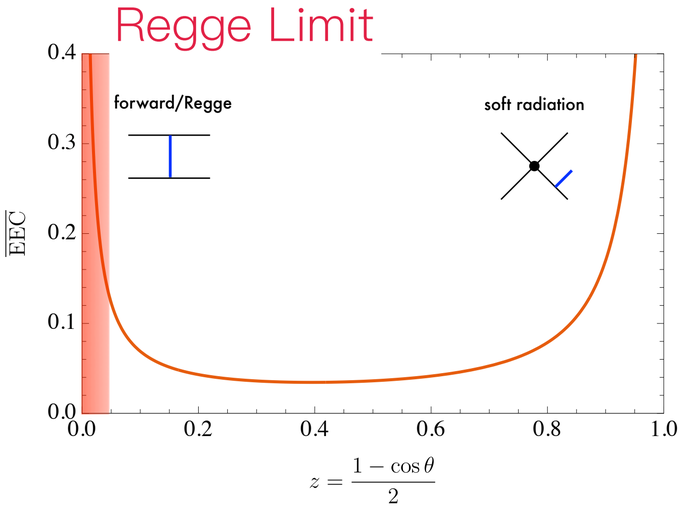

LO beam–averaged EEC of SUGRA

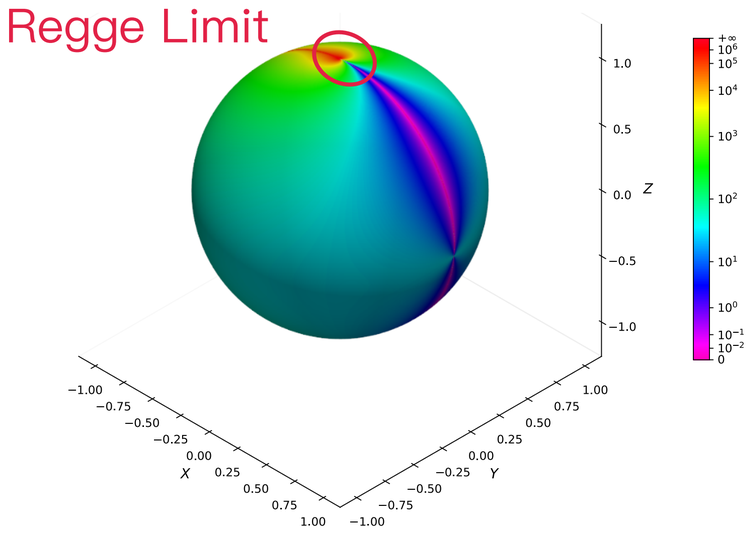

LO celestial EEC of SUGRA

Aside: Related Work

- [Herrmann, Kologlu, Moult, 2412.05384] performed a similar perturbative quantum **gravity** calculation with two incoming scalars and highlighted several future directions.
- [Chicherin, Korchemsky, Sokatchev, Zhiboedov, 2512.23791] extended the setup to **pure gravity and supergravity**, addressing contact terms and IR cancellations, derived an all–order expression in the back–to–back limit governed by universal soft–graviton dynamics, and introduced the ***beam-averaged EEC***.
- [HR, Zheng, Zhu, 2601.21852] further generalized the construction by defining the ***celestial EEC*** with boost–eigenstate initial states, which takes the form of a 4pt function in a fictitious $2d$ CFT on the celestial sphere. We computed it in **(super) Yang–Mills and (super)gravity**, and showed that the $\mathcal{N}=8$ supergravity result can be **bootstrapped**.

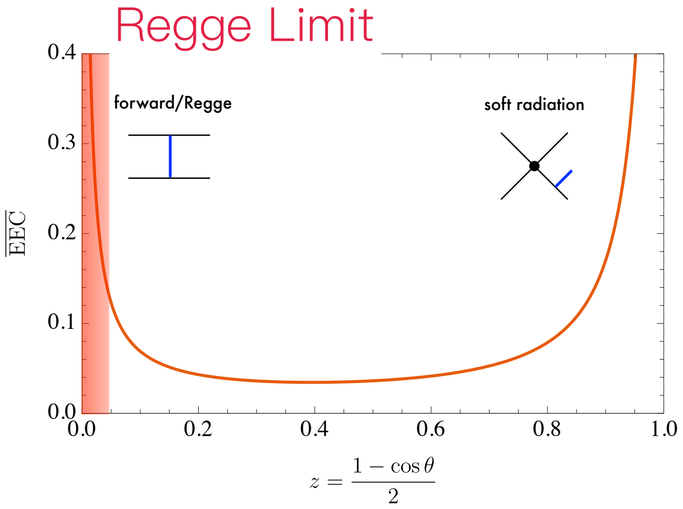

LO beam–averaged EEC of SUGRA

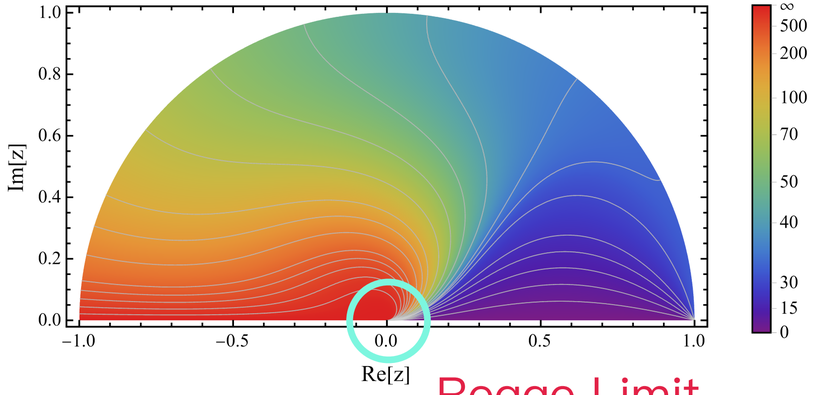

LO celestial EEC of SUGRA

Regge Limit

- Regge limit: $s \gg -t$ [Regge, 1959, 1960]
  (high energy limit, forward scattering limit)
- Highly boosted hadrons collide instantaneously; interesting dynamics on the transverse plane.
- Large logs of $\ln \dfrac{s}{-t}$ come from large **rapidity** gaps between different modes.
- Amplitude level resummation of these logs:
  BFKL equation [Kuraev, Lipatov, Fadin, 1976; Balitsky, Lipatov, 1978; Fadin, Lipatov, 1998]
  Glauber SCET [Gao, Moult, Raman, Ridgway, Stewart, 2024a, b]
- **Goal:** resum analogous rapidity logs $\ln \Delta_\eta$ in EEC in the Regge limit. *In this talk: leading logs.*

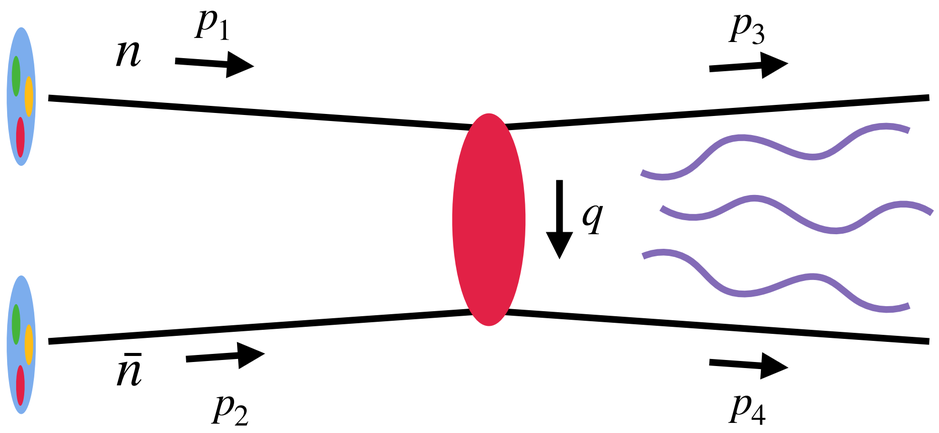

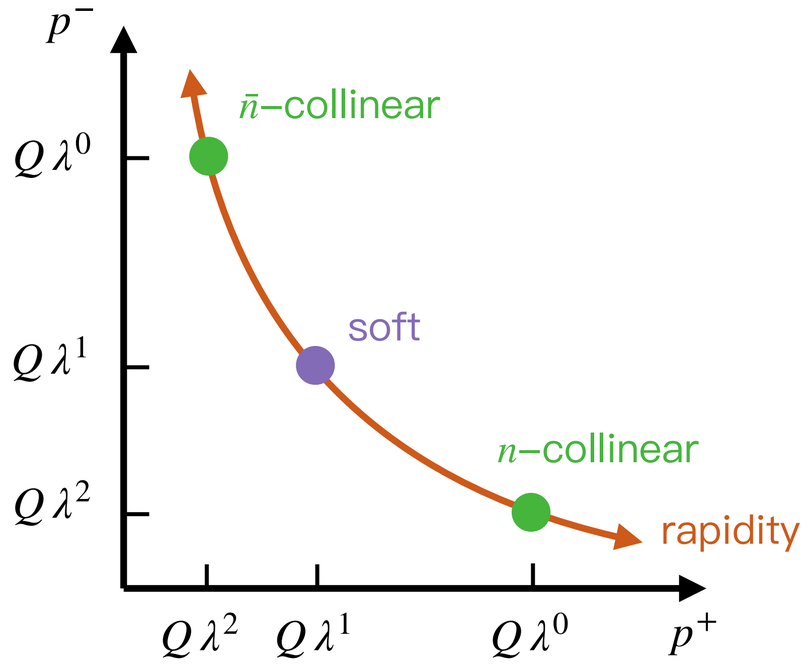

Why EEC for Regge?

- Independent of jet algorithm
  - ➡ Reduced jet-definition systematics (vs jet observables)
- IRC safe; better angular resolution
  - ➡ Improved theory—experiment comparability
- Defined via conserved currents
  - ➡ Smoother transition between parton/hadron regimes
- Inclusive observable
  - ➡ Simpler higher order perturbative calculations
- Natural connection to QFT correlation functions
  - ➡ Access to powerful QFT tools

Aside: Recent Progress

- Many Excellent Talks on EEC, SCET 2026
- DGLAP/BFKL Mixing, Hao Chen, SCET 2025
- Full Range EEC on Tracks, Max Jaarsma, SCET 2025
- Semi-Inclusive Energy Correlators, Hua Xing Zhu, SCET 2024
- …

Perturbative Calculation

Schematically, one has the following factorization formula:

$$\frac{d^2\Sigma_H}{d\Omega_a\, d\Omega_b} = \sum_{\alpha,\beta} \int_0^1 dx_1\, dx_2 f_\alpha(x_1)\, f_\beta(x_2) \boxed{\frac{1}{2s_P} \frac{\langle \alpha(p_1)\, \beta(p_2)\, |\mathcal{E}(n_a)\mathcal{E}(n_b)|\, \alpha(p_1)\, \beta(p_2)\rangle}{\langle \alpha(p_1)\, \beta(p_2)|\alpha(p_1)\, \beta(p_2)\rangle}} \quad \frac{d^2\Sigma_P}{d\Omega_a\, d\Omega_b}$$

The parton level EEC can be calculated perturbatively using a Lorentz invariant formula [HR, Zheng, Zhu, 2026]:

$$\frac{d^2\Sigma_P}{d\Omega_a d\Omega_b} = \frac{1}{8\pi^2 q^2 (n_a\cdot q)^2 (n_b\cdot q)^2} \sum_{n=2}^{\infty} \sum_k \int \frac{d\Pi_n}{\mathrm{sf}_{n,k}}$$

$$\overline{\sum |\mathcal{M}_{2+n,k}|^2} \sum_{i,j=3}^{n+2} (p_i\cdot q)^2 (p_j\cdot q)^2 \delta(p_i\cdot n_a)\delta(p_j\cdot n_b)$$

$q = p_1 + p_2$ is the parton c.m. energy.

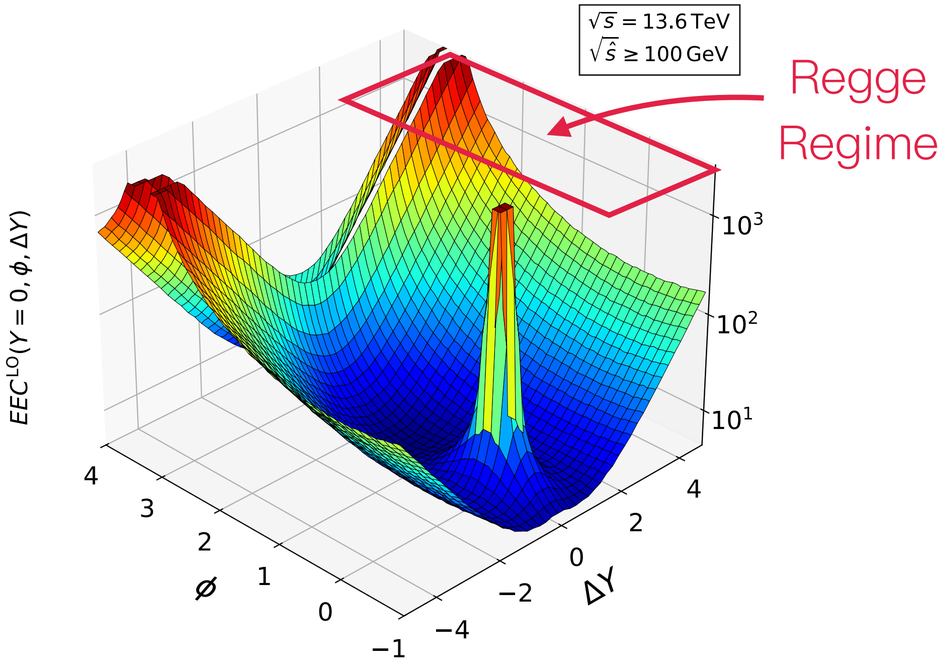

LO EEC for proton collisions

Warm Up: Rapidity Logs in EEC

Regge regime: large detector rapidity separation: $\Delta_\eta \gg 1$.

Rapidity logs $\ln \Delta_\eta$ appear at each perturbative order.

e.g. gg→ggg gives $\dfrac{d^2\Sigma_P}{d\Omega_a d\Omega_b} \xrightarrow{\Delta_\eta \to \infty} \dfrac{3N_c^2 (N_c^2-1)\,\alpha_s^3\,\eta\,\Delta_\eta^3 \ln \Delta_\eta}{(32\pi)^2\left(1+2\eta\cos\phi+\eta^2\right)}$

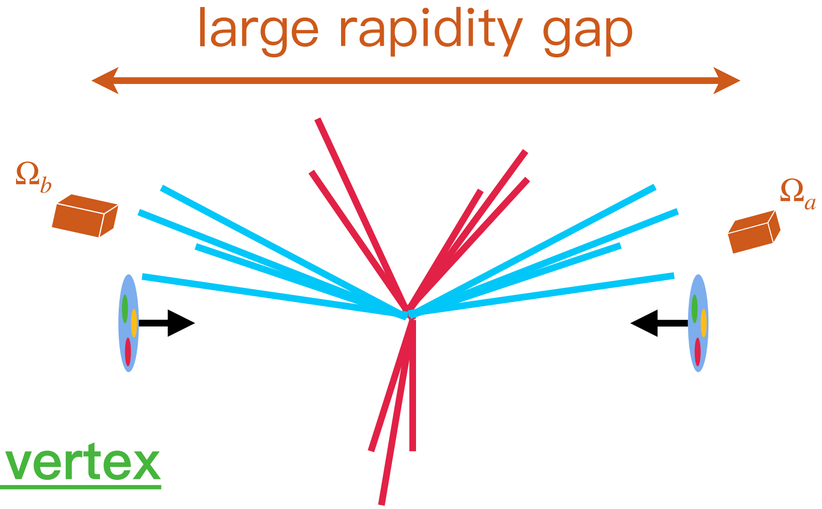

At this order, the $\ln \Delta_\eta$ term is captured by Lipatov's effective vertex

[Lipatov, 1995]

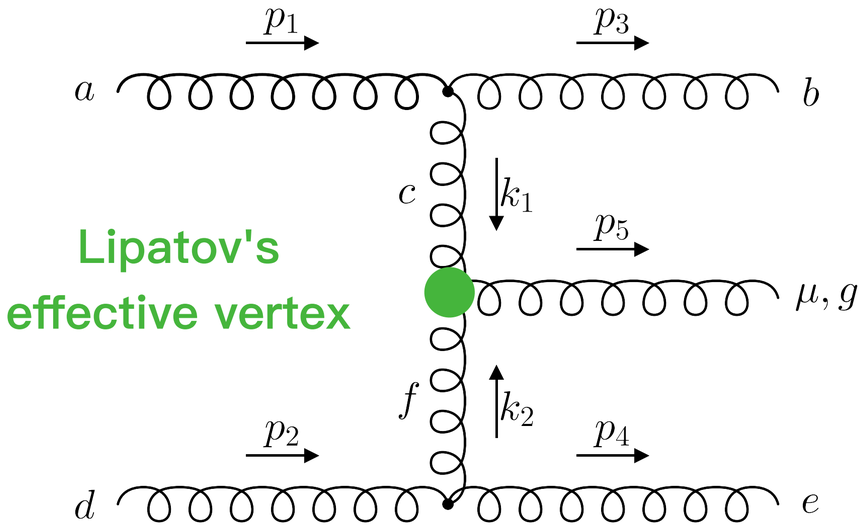

Lipatov's effective vertex

$$iM^\mu = \frac{2g^3}{s} f_{abc} f_{def} f_{cfg} \eta^{h_1 h_3} \eta^{h_2 h_4} \Gamma^\mu(k_1, k_2)$$

$$\Gamma^\mu(k_1,k_2) = \frac{1}{\lambda_1 \rho_2}\left(\left(\rho_1 + \frac{2\lambda_1}{\lambda_2}\right)p_1^\mu - \left(\lambda_2 + \frac{2\rho_2}{\rho_1}\right)p_2^\mu - k_{1\perp}^\mu + k_{2\perp}^\mu\right)$$

- Sudakov decomposition: $k_i^\mu = \rho_i p_1^\mu + \lambda_i p_2^\mu + k_{i\perp}^\mu$
- Regge limit: $1 \gg |\rho_1| \gg |\rho_2|,\ 1 \gg |\lambda_2| \gg |\lambda_1|$

Lipatov

Multi Regge Kinematics

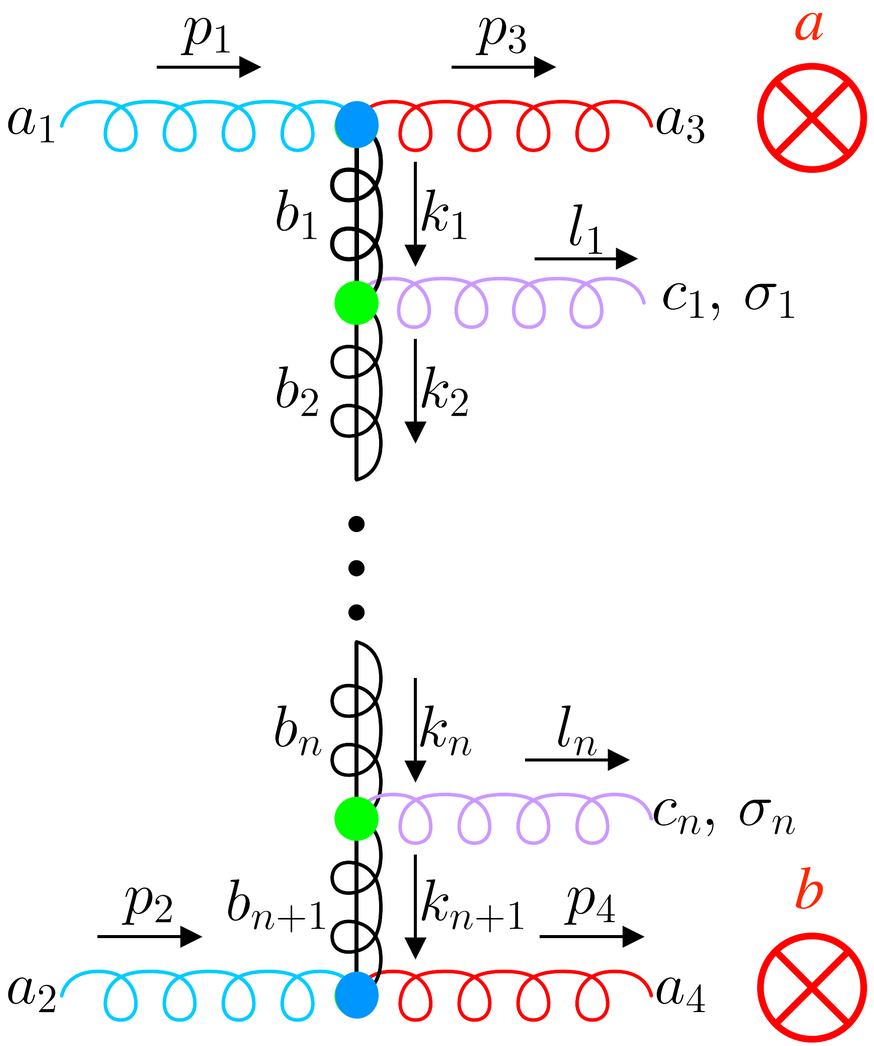

n–th ladder diagram

At higher perturbative orders, leading rapidity logs arise from Multi Regge Kinematics (MRK):

$$\rho_0 \equiv 1 \gg \rho_1 \gg \cdots \gg \rho_{n+1}, \quad |\lambda_{n+2}| \equiv 1 \gg |\lambda_{n+1}| \gg \cdots \gg |\lambda_1|$$

Kinematics

- On shell condition:

  $$\left(\vec{k}_{i\perp} - \vec{k}_{i+1\perp}\right)^2 \approx -\rho_i \lambda_{i+1} s, \quad \vec{k}_{1\perp}^2 \approx -\lambda_1 s, \quad \vec{k}_{n+1\perp}^2 \approx \rho_{n+1} s$$

- The transverse momentum of real radiation are of the same order: $l_{i\perp}^2 \sim p_{3,\perp}^2 \sim p_{4,\perp}^2 \sim -\rho_i \lambda_{i+1} s \sim -t$
- Detectors' rapidities help fix: $-\lambda_1 \approx \dfrac{1}{\eta \Delta_\eta}, \rho_{n+1} \approx \dfrac{\eta}{\Delta_\eta}$
- Logs of $\ln \dfrac{s}{-t}$ now become logs of $\ln \Delta_\eta$
- Detectors' azimuthal angles help fix $\vec{k}_{1\perp}, \vec{k}_{n+1\perp}$

Multi Regge Kinematics

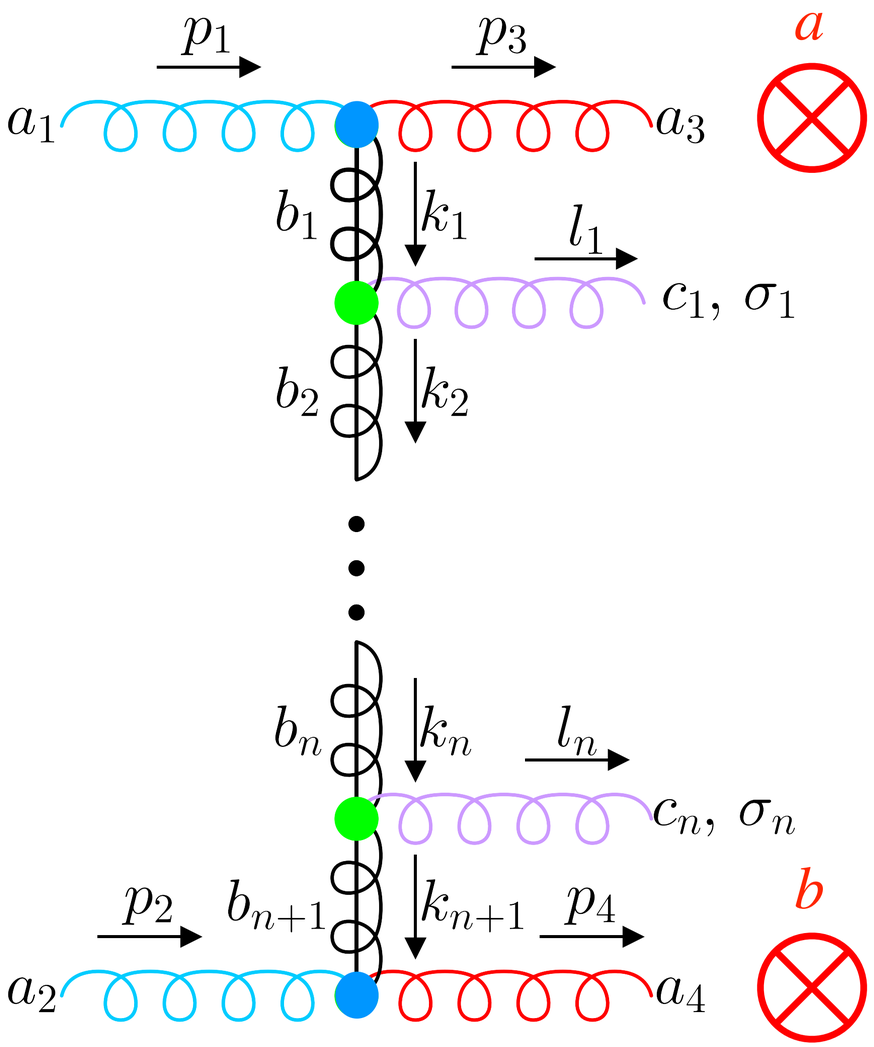

n–th ladder diagram

At higher perturbative orders, leading rapidity logs arise from Multi Regge Kinematics (MRK):

$$\rho_0 \equiv 1 \gg \rho_1 \gg \cdots \gg \rho_{n+1}, \quad |\lambda_{n+2}| \equiv 1 \gg |\lambda_{n+1}| \gg \cdots \gg |\lambda_1|$$

Dynamics (Feynman Rules)

- ●: eikonal vertex (polarization vector dotted in)

$$2gf_{a_1a_3b_1}\eta^{h_1h_3}p_1^\mu, \qquad 2gf_{a_2a_4b_{n+1}}\eta^{h_2h_4}p_2^\mu$$

- ●: Lipatov's effective vertex

$$\Gamma_i^\mu(k_i,k_{i+1}) = \frac{1}{\lambda_i\rho_{i+1}}\left(\left(\rho_i+\frac{2\lambda_i}{\lambda_{i+1}}\right)p_1^\mu - \left(\lambda_{i+1}+\frac{2\rho_{i+1}}{\rho_i}\right)p_2^\mu - k_{i\perp}^\mu + k_{i+1\perp}^\mu\right)$$

- b_i k_i: reggeized gluon $\tilde{D}_{\mu\nu}\left(\hat{s}_i,\vec{k}_{i\perp}^2\right) = \frac{ig_{\mu\nu}}{\vec{k}_{i\perp}^2}\left(\frac{\rho_{i-1}}{\rho_i}\right)^{\epsilon_G\left(\vec{k}_{i\perp}^2\right)}$

$$\epsilon_G\left(\vec{k}_{i\perp}^2\right) = -N_c\,\alpha_s\int\frac{d^2\vec{k}_\perp}{(2\pi)^2}\frac{2\,\vec{k}_{i\perp}^2}{\left(\vec{k}_{i\perp}-\vec{k}_\perp\right)^2\left(\vec{k}_\perp^2+\left(\vec{k}_{i\perp}-\vec{k}_\perp\right)^2\right)}$$

divergent!

Multi Regge Kinematics

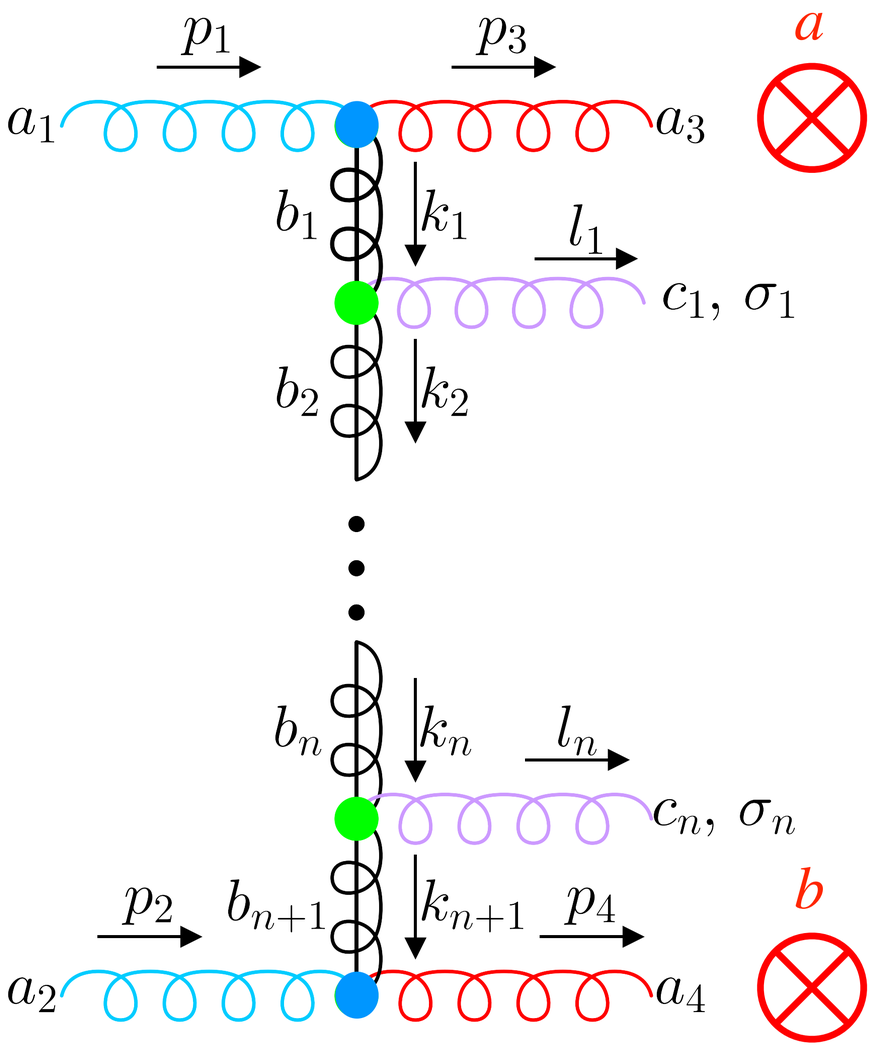

n–th ladder diagram

At higher perturbative orders, leading rapidity logs arise from Multi Regge Kinematics (MRK):

$$\rho_0 \equiv 1 \gg \rho_1 \gg \cdots \gg \rho_{n+1}, \quad |\lambda_{n+2}| \equiv 1 \gg |\lambda_{n+1}| \gg \cdots \gg |\lambda_1|$$

Amplitude

The n–th ladder diagram amplitude then reads:

$$\overline{\sum |M_{2\to 2+n}|^2} = C_{r1}C_{r2}\,(N_c^2-1)\,\pi^2\alpha_s^2 \left(\frac{16\pi N_c\,\alpha_s}{s}\right)^n \left(\prod_{i=1}^{n}\frac{s}{\left(\vec{k}_{i\perp}-\vec{k}_{i+1\perp}\right)^2}\right)\left(\prod_{i=1}^{n+1}\left(\frac{\rho_{i-1}}{\rho_i}\right)^{2\epsilon_G\left(\vec{k}_{i\perp}^2\right)}\right)$$

color factor for gluon/quark line

potential logs

Divergence in $\epsilon_G(k_i^2)$ should cancel after phase space integration.

EEC in MRK

In the parton c.m. frame, the phase space integration reduce to a simpler form in MRK:

nested integral

$$\frac{d^2\Sigma_P}{d\Omega_a d\Omega_b} = \sum_{n=0}^{\infty} \frac{s}{(32\pi)^2} \left(\prod_{i=2}^{n+1} \int \frac{d^2\vec{k}_{i,\perp}^2}{2(2\pi)^3} \right) \left(\prod_{i=1}^{n} \int_0^1 \frac{d\rho_i}{\rho_i} \right) \int_0^1 d\rho_{n+1} \overline{\sum |M_{2\to 2+n}|^2} \delta\left(\rho_{n+1} - \frac{1}{\Delta\eta}\right) \delta^2\left(\vec{k}_{n+1,\perp} - \vec{k}_b\right)$$

$$f_n(\vec{k}_a, \vec{k}_b, s) \equiv \tilde{f}_n\left(\eta = \frac{|\vec{k}_b|}{|\vec{k}_a|}, \Delta_\eta = \frac{s}{|\vec{k}_a||\vec{k}_b|}, \phi = \phi_a - \phi_b - \pi\right)$$

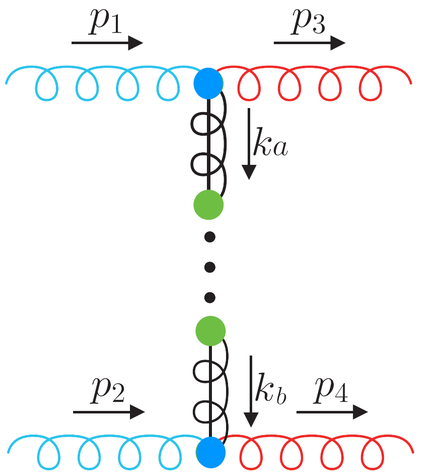

After introducing $\tau_i \equiv \rho_i/\rho_{i-1}$, the nested integral simplifies in Mellin space:

$$F_n\left(\vec{k}_a, \vec{k}_b, \omega\right) = \frac{1}{s^3} \int_1^\infty d\Delta_\eta \, \Delta_\eta^{-\omega-1} f_n(\vec{k}_a, \vec{k}_b, s) \quad \Longleftrightarrow \quad f_n(\vec{k}_a, \vec{k}_b, s) = s^3 \int_C \frac{d\omega}{2\pi i} \Delta_\eta^\omega F_n\left(\vec{k}_a, \vec{k}_b, \omega\right)$$

Potential logs then become Mellin poles $\left(\frac{\rho_{i-1}}{\rho_i}\right)^{2\epsilon_G(k_i^2)} \Longleftrightarrow \frac{1}{\omega - 2\epsilon_G(k_i^2)}$

Evolution Equation

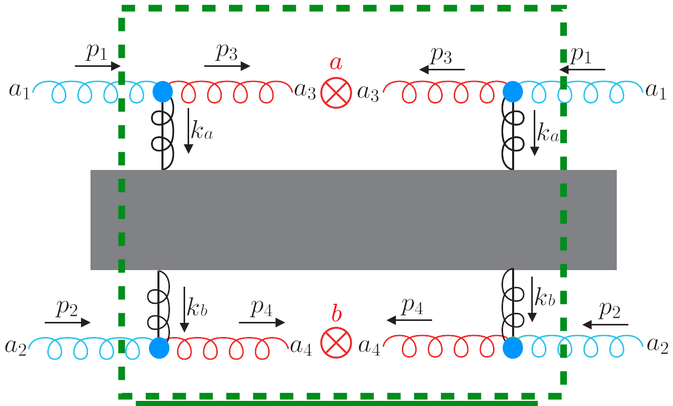

=

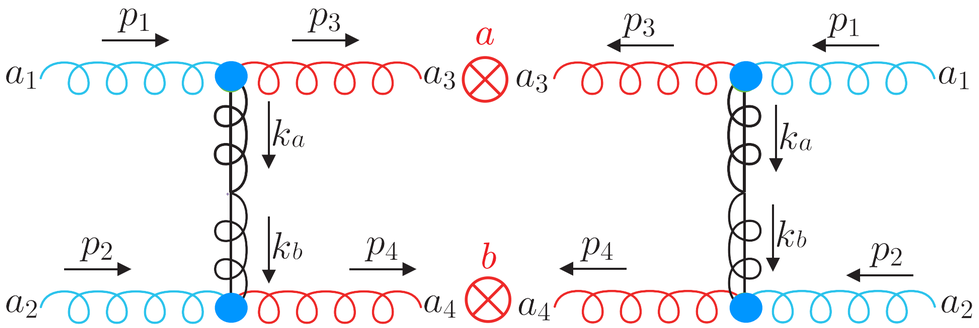

+

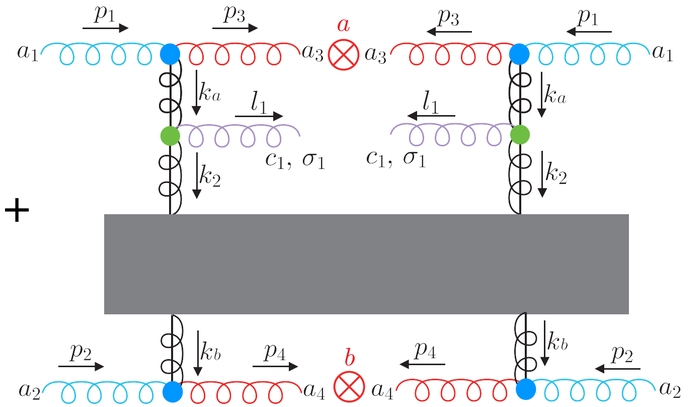

$$\omega F\left(\vec{k}_a,\vec{k}_b,\omega\right)=\frac{C_{r1}C_{r2}(N_c^2-1)\,\alpha_s^2}{1024\,k_a^2k_b^2}\,\delta^{(2)}\left(\vec{k}_a-\vec{k}_b\right)+\frac{N_c\,\alpha_s}{\pi^2}\int d^2\vec{k}\,\frac{1}{(\vec{k}-\vec{k}_a)^2}\left[\frac{k^2}{k_a^2}F(\vec{k},\vec{k}_b,\omega)-\frac{k_a^2}{k^2+(\vec{k}-\vec{k}_a)^2}F(\vec{k}_a,\vec{k}_b,\omega)\right]$$

Redefine: $G(\vec{k}_a,\vec{k}_b,\omega)\equiv\dfrac{1024\,k_a^2k_b^2}{C_{r1}C_{r2}(N_c^2-1)\alpha_s^2}F(\vec{k}_a,\vec{k}_b,\omega)$

Vanish as $\vec{k}\to\vec{k}_a$, manifestly convergent

$$\omega G(\vec{k}_a,\vec{k}_b,\omega)=\delta^{(2)}(\vec{k}_a-\vec{k}_b)+\frac{N_c\,\alpha_s}{\pi^2}\int\frac{d^2\vec{k}}{(\vec{k}_a-\vec{k})^2}\left[G(\vec{k},\vec{k}_b,\omega)-\frac{k_a^2}{k^2+(\vec{k}-\vec{k}_a)^2}G(\vec{k}_a,\vec{k}_b,\omega)\right]$$

LL BFKL equation with zero momentum transfer

Leading Log Resummation

Solving the BFKL equation gives a Fourier mode expansion of the EEC:

$$\frac{d^2\Sigma_P}{d\Omega_a\, d\Omega_b} = \frac{C_{r1}C_{r2}\left(N_c^2-1\right)\alpha_s^2}{1024}\,\Delta_\eta^3 \sum_{n=0}^{\infty} \frac{\cos\left(n(\phi-\pi)\right)}{1+\delta_{0n}} \int_{-\infty}^{+\infty} \eta^{-2i\nu}\,\Delta_\eta^{\frac{N_c\alpha_s}{\pi}\chi_n(\nu)}\,d\nu$$

Direct connection to BFKL eigenfunctions!

Each Fourier mode is a BFKL eigenfunction, with eigenvalue

$$\chi_n(\nu) = -2\gamma_E - 2\Re\left(\mathrm{Li}_2\left(\frac{n+1}{2}+i\nu\right)\right)$$

The maximum of $\chi_n(\nu)$ determines the hard Pomeron intercept:

$$\alpha(0) = 1+\frac{N_c\alpha_s}{\pi}\chi_0(0) = 1+\frac{4N_c\alpha_s}{\pi}\ln 2$$

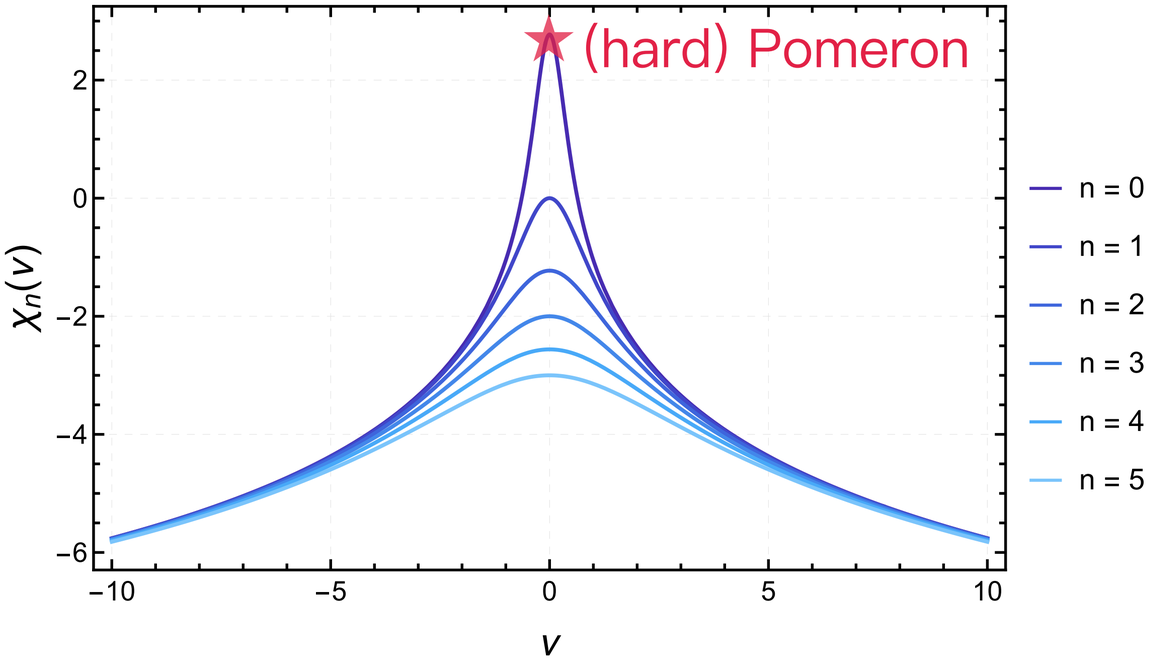

Behavior of BFKL eigenvalue $\chi_n(\nu)$

LL EEC at Parton Level

- Leading Fourier modes A_n^{LL} grow asymptotically with ΔY (higher Fourier modes can decrease)
- The leading growth is dominated by the $n = 0$ mode (hard Pomeron)
- Effective growth rate decreases ***monotonically*** with n, mirroring the BFKL eigenvalue hierarchy:
  larger $n \Rightarrow$ smaller effective intercept $\Rightarrow$ weaker ΔY evolution
- Normalized to A_0^{LL}, higher harmonics are progressively damped as ΔY increases
  $\Longrightarrow$ angular structure is washed out at large ΔY

Y=0

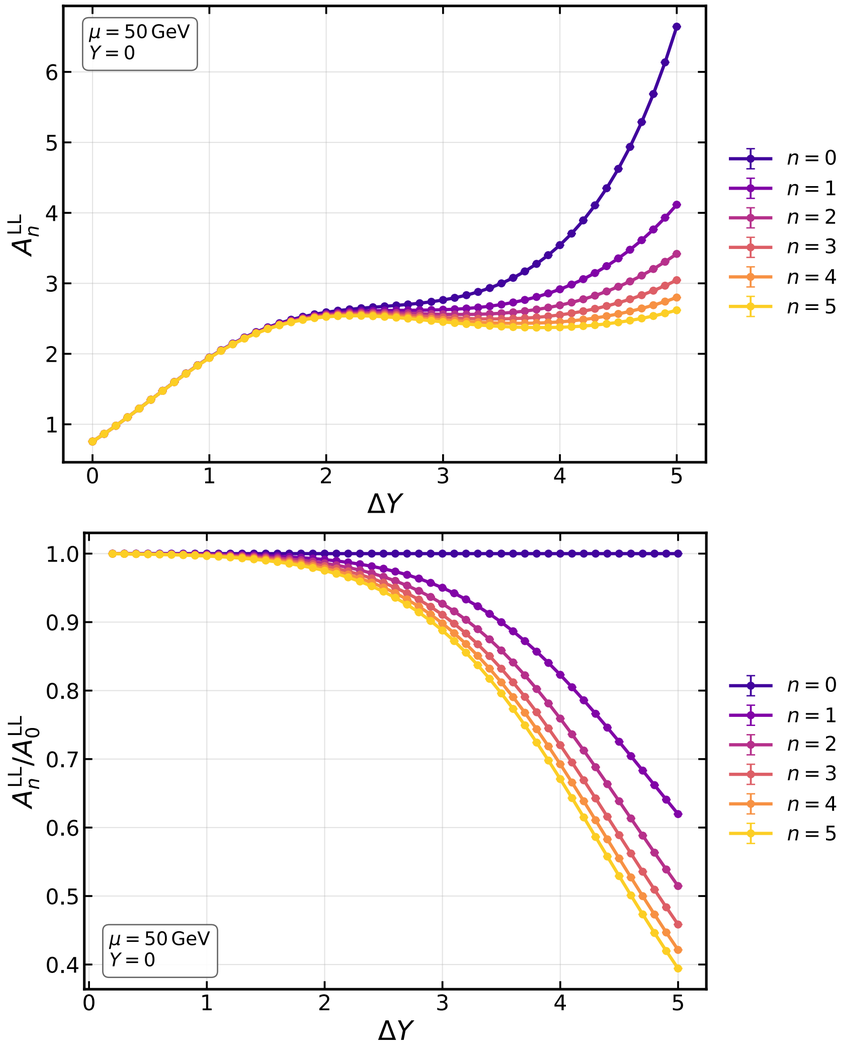

LL EEC at Parton Level

- Leading Fourier modes A_n^{LL} grow asymptotically with ΔY (higher Fourier modes can decrease)
- The leading growth is dominated by the $n = 0$ mode (hard Pomeron)
- Effective growth rate decreases ***monotonically*** with n, mirroring the BFKL eigenvalue hierarchy:
  larger $n \Rightarrow$ smaller effective intercept $\Rightarrow$ weaker ΔY evolution
- Normalized to A_0^{LL}, higher harmonics are progressively damped as ΔY increases
  $\Longrightarrow$ angular structure is washed out at large ΔY
- The same trends hold for different Y

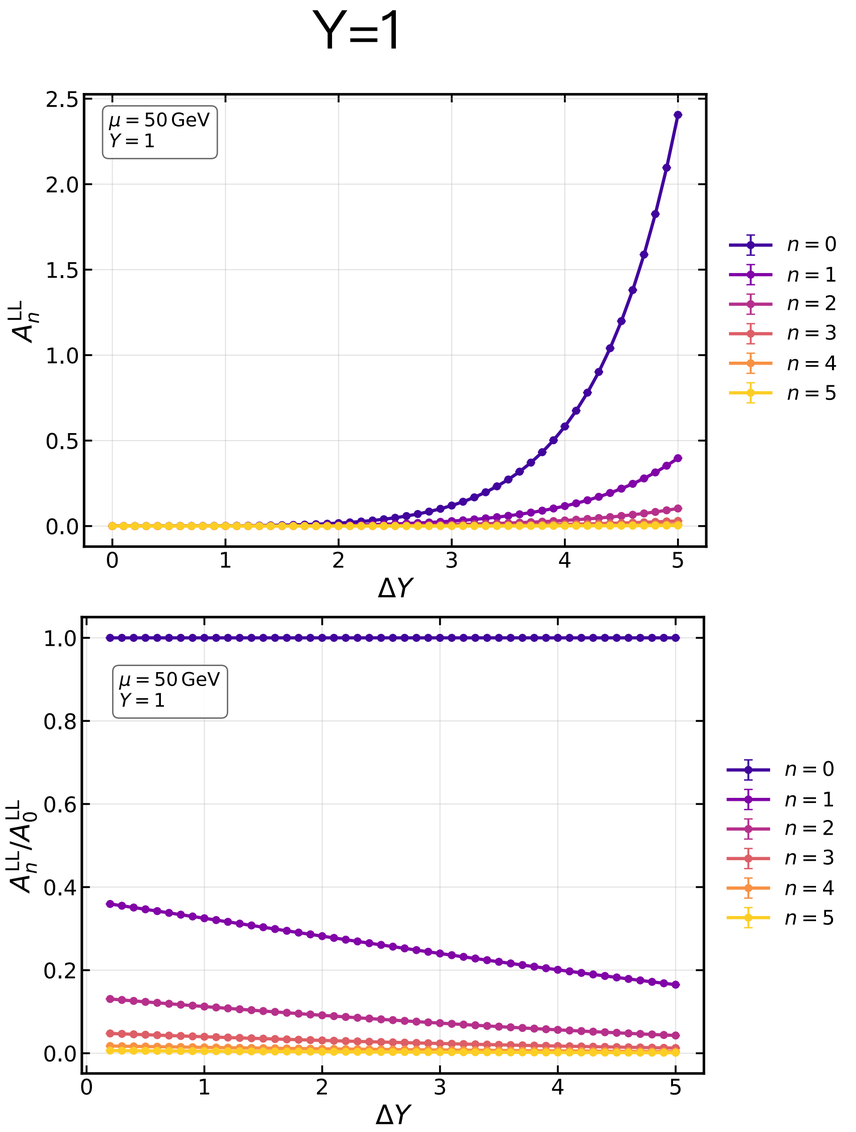

LL EEC at Parton Level

In the Regge regime (sufficiently large ΔY), the EEC can be well approximated by a ***truncated*** Fourier expansion. This reveals the evolution of the azimuthal correlation with ΔY.

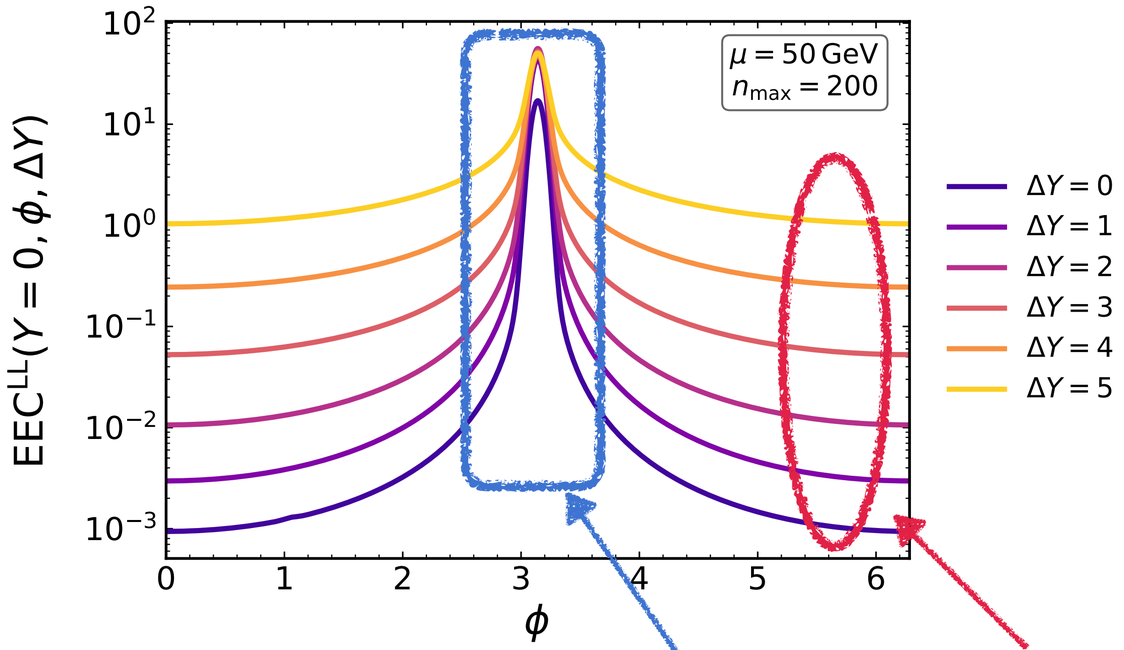

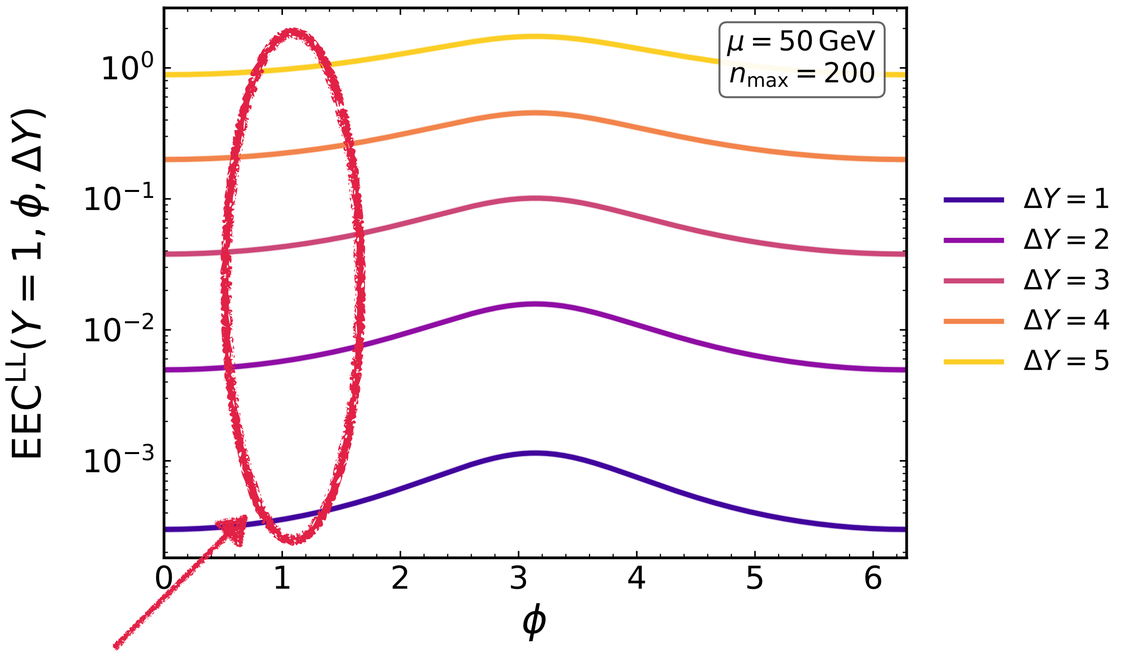

As ΔY grows:

Near–side plateau increases

Azimuthal decorrelation increases

Away–side peak broadens

LL EEC with PDFs

Recall the parton level Fourier expansion (LL):

$$\frac{d^2\Sigma_P}{d\Omega_a\, d\Omega_b} = \frac{C_{r1}C_{r2}\left(N_c^2-1\right)\alpha_s^2}{1024}\,\Delta_\eta^3 \sum_{n=0}^{\infty} \frac{\cos\left(n(\phi-\pi)\right)}{1+\delta_{0n}} \int_{-\infty}^{+\infty} \eta^{-2i\nu}\,\Delta_\eta^{\frac{N_c\alpha_s}{\pi}\chi_n(\nu)}\, d\nu$$

only channel dependent factor

Δ_η and ϕ are boost invariant, while η is frame dependent

Hadronic initial state:

exp. friendly rep. Jacobian color weighted parton luminosity

$$\frac{d^3\Sigma_H}{dY\, d\Delta Y\, d\phi} = \frac{16\pi\eta^2\Delta_\eta^2}{(\eta+\Delta_\eta)^2(1+\eta\,\Delta_\eta)^2}\left(C_A^2\, g_1 g_2 + C_A\, C_F\,(g_1 q_2 + q_1 g_2) + C_F^2\, q_1 q_2\right)$$

$$\otimes \frac{x_1^3\, x_2^3}{(x_1\,\Delta_\eta + x_2\,\eta)^3\,(x_1 + x_2\,\eta\,\Delta_\eta)^3} \frac{d^2\Sigma_P}{d\Omega_a d\Omega_b}\left(\hat{\eta} = \frac{x_2}{x_1}\eta, \Delta_\eta, \phi\right) + \mathcal{O}\left(\frac{\Lambda_{QCD}}{Q}\right)$$

frame transformation factor rapidity shift

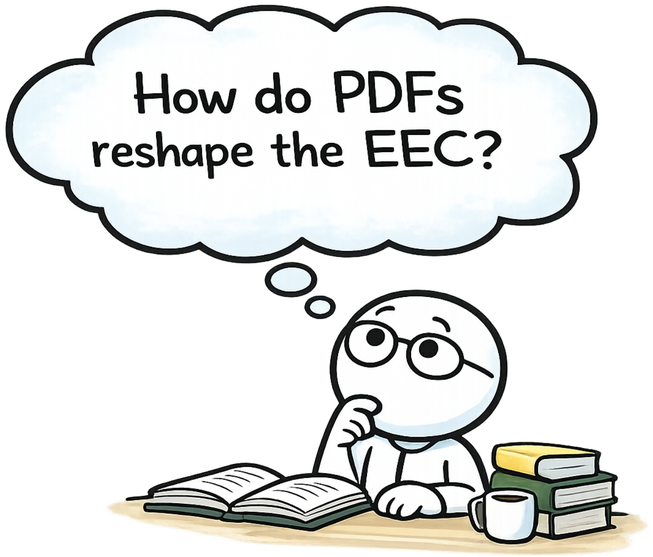

LL EEC with PDFs

Similar to the Parton Level!

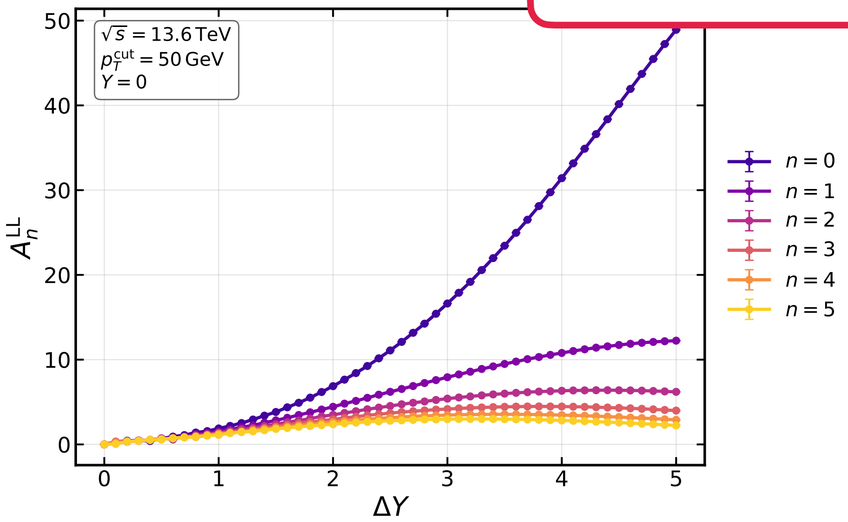

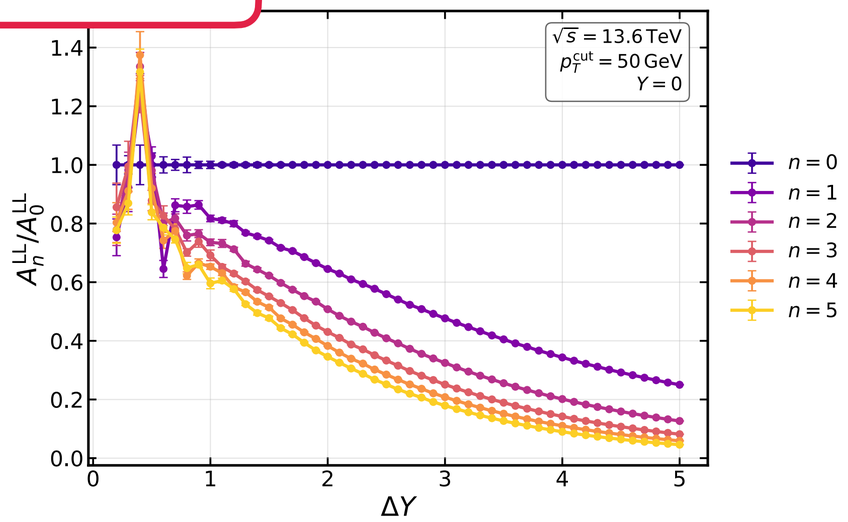

$$\mu = \sqrt{\frac{\hat{s}}{\Delta_\eta}} \sim k_a, k_b \geq p_T^{cut}$$

- Same ΔY trend as parton level;

  Near–side plateau still rises with ΔY
- PDF convolution “tenders” the away–side peak

  $\Longrightarrow$ decorrelation more manifest
- $n = 0$ mode (Pomeron) dominance enhanced

  $\Longrightarrow$ angular structure washed out at large ΔY

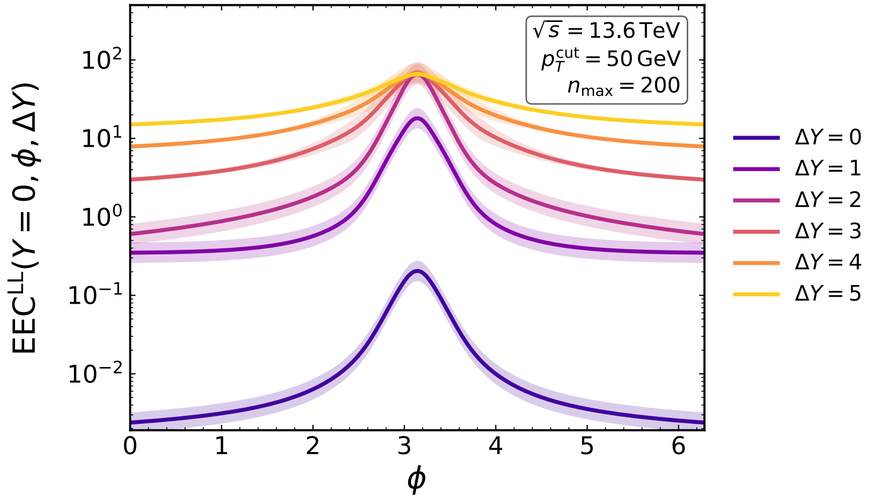

Pythia Data vs LL Prediction

- **Goal:** probe BFKL dynamics via the EEC at hadron colliders in the Regge regime.
- **Validation step:** compare our LL prediction to Pythia simulations.
- **Caveat:** BFKL resummation is **not** implemented in PYTHIA; PYTHIA serves as a **baseline**.
- **Event selection:** dijet events at $\sqrt{s} = 13.6\,\text{TeV}$ with $p_T^{jet} \geq 50\,\text{GeV}$ (anti–k_T, $R = 0.4$).

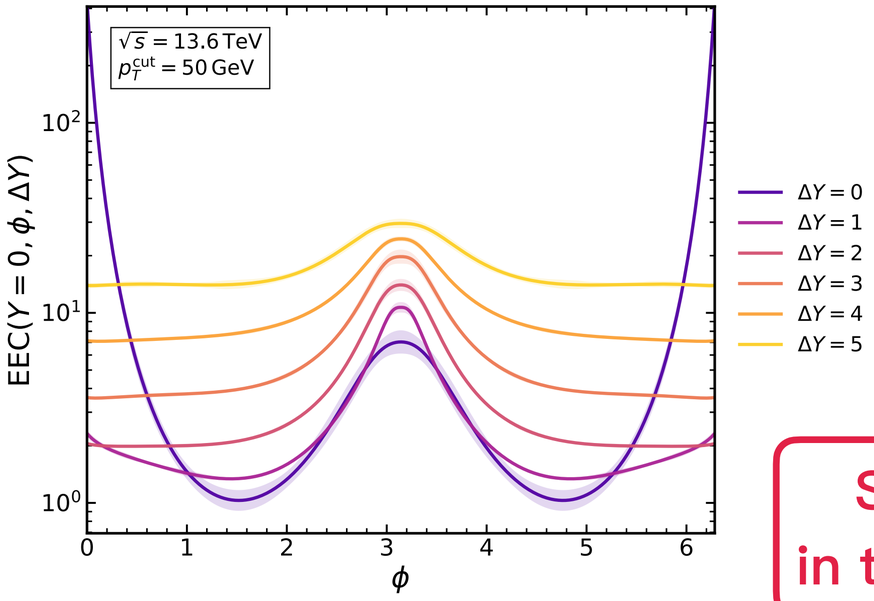

Pythia Data

Similar Behavior in the Regge Regime

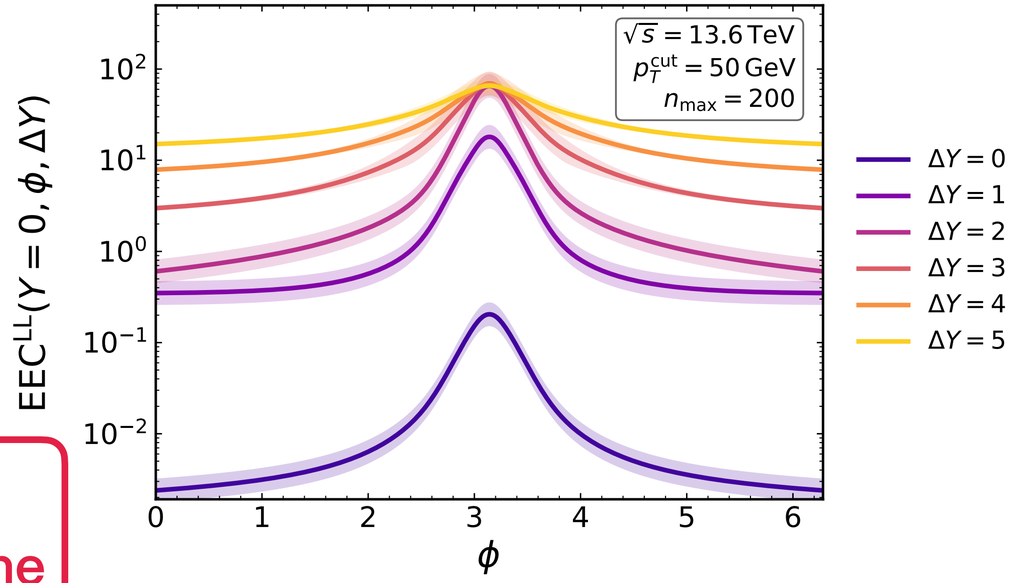

LL Prediction

Pythia Data vs LL Prediction

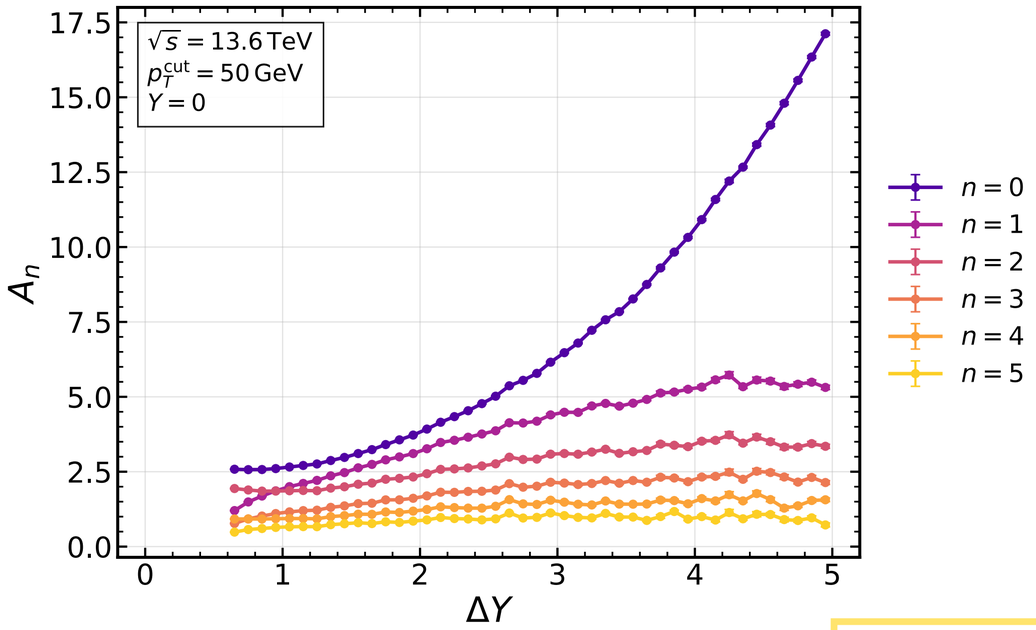

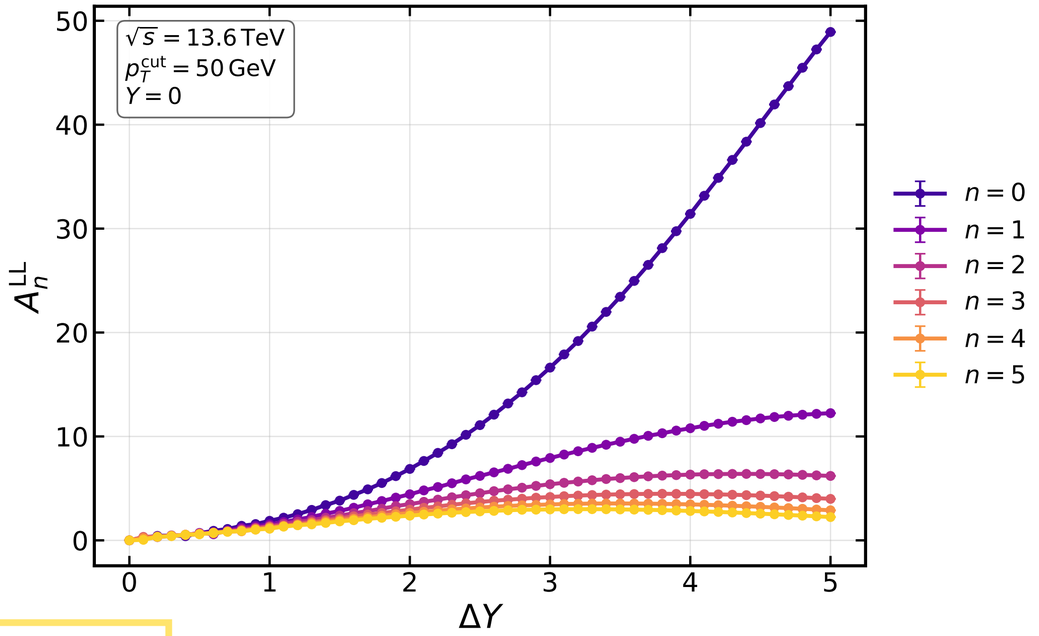

Pythia Data ◀ ····· Normalization depends on event selection and cuts ····· LL Prediction

Robust Similarities:

- Pythia and LL show similar ΔY scaling
- $n = 0$ mode (Pomeron) dominates and grows rapidly with ΔY
- Higher modes saturate into plateaus at large ΔY, with lower plateaus for larger n

Pythia Data vs LL Prediction

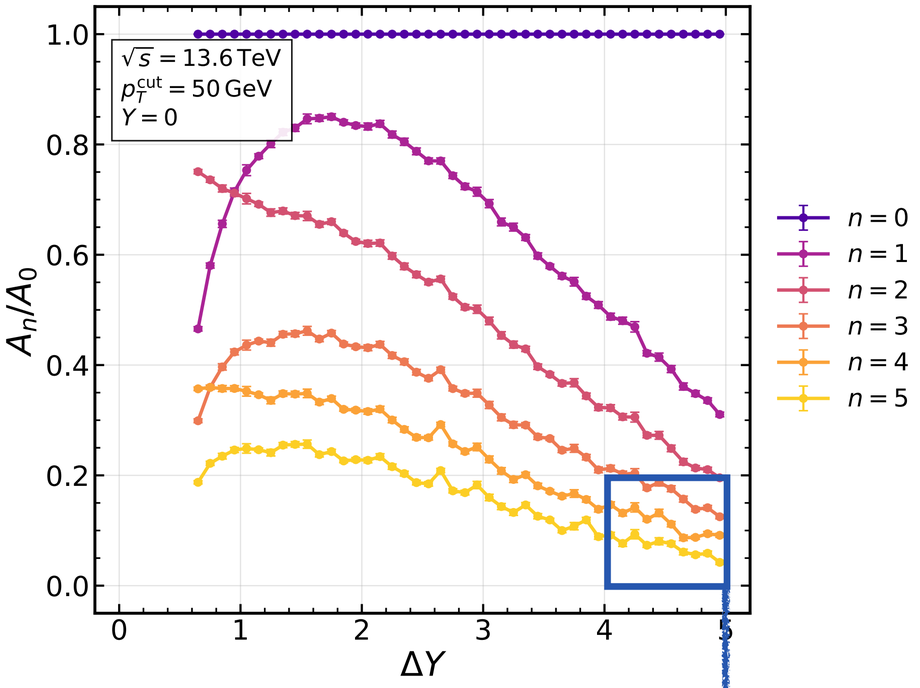

Pythia Data

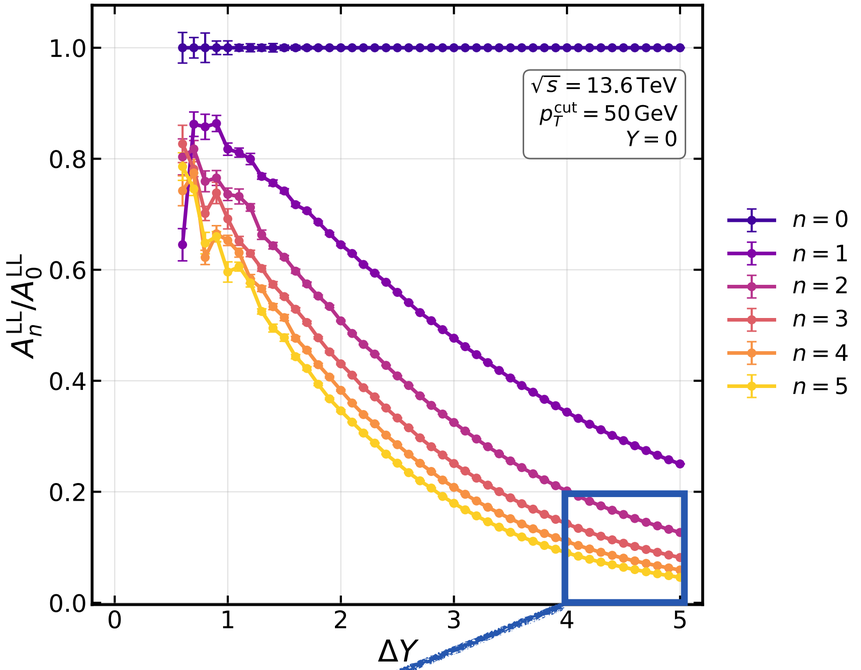

LL Prediction

LL predicts a steeper fall of the ratios.
In this window, Pythia is nearly linear,
while LL shows a downward curvature.

Summary & Outlook

- We propose to measure the EEC in the Regge regime at hadron colliders as a clean probe of BFKL dynamics.
- We derive a rapidity evolution equation and resum LL via the BFKL solution.
- The result is a Fourier expansion, with eigenvalues controlling the ΔY evolution.
- Pythia and LL share ***robust*** similarities in ΔY scaling, with residual LL deviations offering a potential BFKL signal.
  - Factorization formula using SCET: soft & collinear functions + detectors.
  - NLL accuracy: NLL BFKL + running coupling + NLO collinear functions.
  - Operator language for the Pomeron: Wilson lines/light ray operators.

Thank you for your attention!

Backup: celestial EEC

Celestial EEC: $$\frac{d^2\Sigma^{(J_1,J_2)}}{d\Omega_a d\Omega_b} = \mathrm{Tr}\left[\mathcal{E}(n_a)\mathcal{E}(n_b)\mathbb{P}_1^{J_1}(n_1)\mathbb{P}_2^{J_2}(n_2)\right]$$

Beam Operator (boost eigenstate): $$\mathbb{P}^{(J)}(n) = \int_0^\infty \frac{dP}{P}\, P^{-J}\frac{|P\rangle\langle P|}{\langle P|P\rangle}$$

Differential in c.m. energy squared:

$$\frac{d^3\Sigma^{(J_1,J_2)}}{d\Omega_a\, d\Omega_b\, dq^2} = \left(\frac{2n_1\cdot n_2}{q^2}\right)^{\frac{J_1+J_2}{2}} \frac{(n_1\cdot n_a)^{\frac{J_1-J_2}{2}}}{4(n_a\cdot n_b)^3(n_2\cdot n_a)^{\frac{J_1-J_2}{2}}} G^{(J_1,J_2)}(u,v)$$

can be extracted from EEC by integrating over rapidity

Behaves just like 4pt function in fictitious $2d$ CFT!

Cross Ratios: $$u = z\bar{z} = \frac{(n_a\cdot n_2)(n_b\cdot n_1)}{(n_a\cdot n_1)(n_b\cdot n_2)}$$

$$v = (1-z)(1-\bar{z}) = \frac{(n_a\cdot n_b)(n_1\cdot n_2)}{(n_a\cdot n_1)(n_b\cdot n_2)}$$

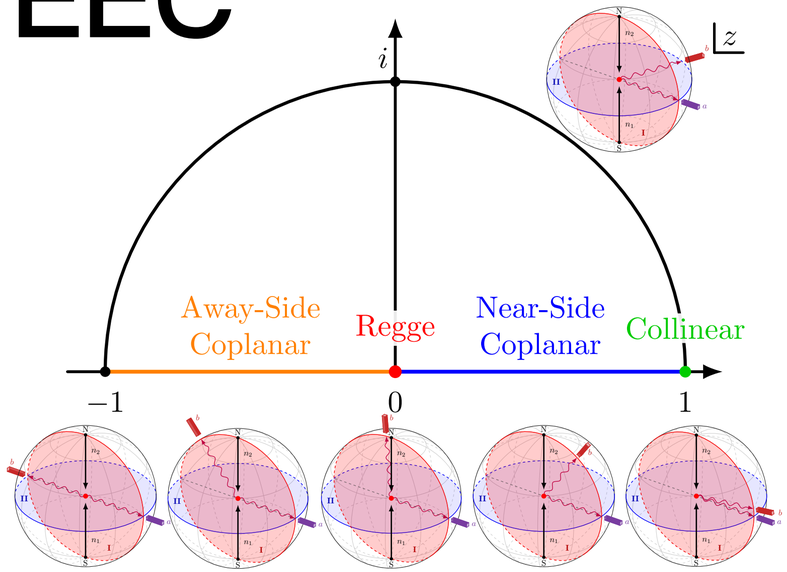

All information of the cEEC is contained in the upper half unit disc for $J_1 = J_2$

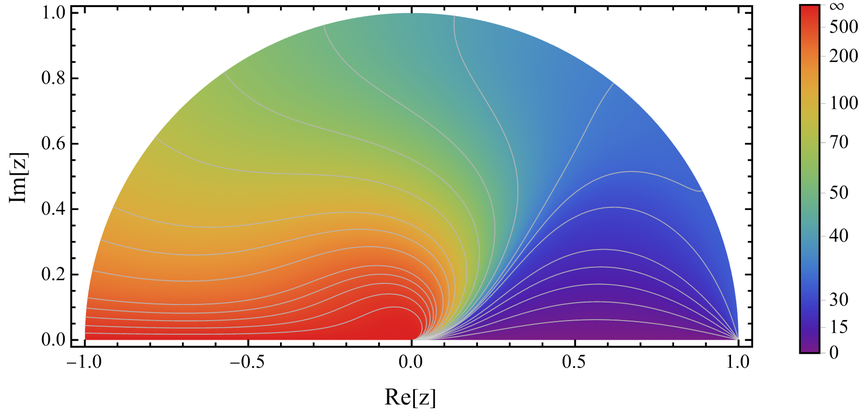

Leading order $\mathbf{cEEC}^{(0,0)}_{\mathrm{SUGRA}}(z,\bar{z})$ result

Backup: LO Prediction

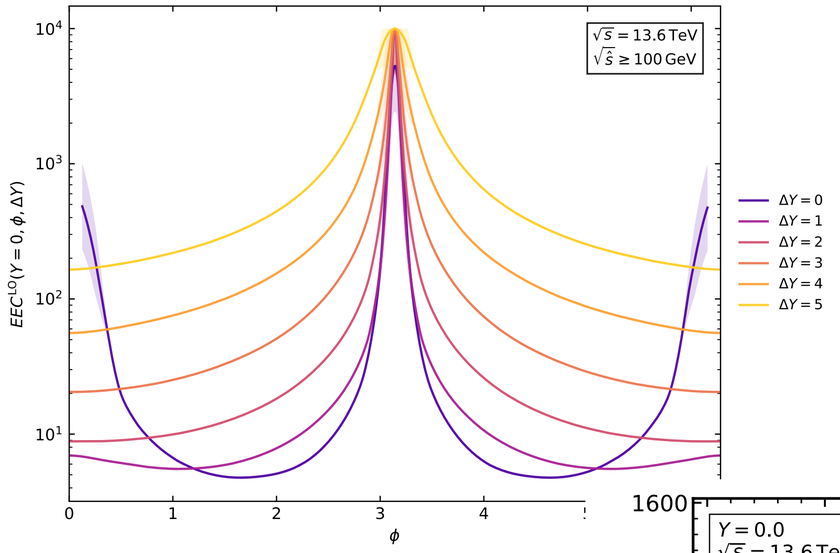

- The LO away-side peak is much sharper than in Pythia data and the LL prediction.
- To extract stable Fourier modes, we truncate the distribution in the away-side region, cutting out $|\phi - \pi| < 0.1$

In the Regge regime, LO differs markedly from both Pythia and LL, as clearly seen in the plots.